ELSEVIER
www.elsevier.com/locate/ica
Inorganica Chimica Acta 327 (2002) 169–178
Inorganica Chimica Acta

# Heptacoordinate dithiophosphate W(II) and Mo(II) complexes of diphosphines and iodide

Huizhang Liu [a], Maria José Calhorda [a,b,*], Vitor Félix [c], Michael G.B. Drew [d], Luís F. Veiros [e]

[a] *Instituto de Tecnologia Química e Biológica (ITQB), Av. da República, EAN, Apt 127, 2781-901 Oeiras, Portugal*
[b] *Departamento de Química e Bioquímica, Faculdade de Ciências da Universidade de Lisboa, 1749-016 Lisbon, Portugal*
[c] *Departamento de Química, Universidade de Aveiro, 3810-193 Aveiro, Portugal*
[d] *Department of Chemistry, University of Reading, Whiteknights, Reading, RG6 6AD, UK*
[e] *Centro de Química Estrutural, Complexo I, Instituto Superior Técnico, Av. Rovisco Pais, 1, 1049-001 Lisbon, Portugal*

Received 25 June 2001; accepted 29 August 2001

Dedicated to Professor K. Vrieze on the occasion of his retirement

---

**Abstract**

New complexes $[MI(CO)_2(dppe)\{S_2P(OEt)_2\}]$ (M = W, **1a**; M = Mo, **1b**), $[MI(CO)_2(dppm)\{S_2P(OEt)_2\}]$ (M = W, **2a**; M = Mo, **2b**) and $[W(CO)(dppe)\{S_2P(OEt)_2\}_2][O_2dppe]$ (**3a**), were synthesised from $[MI_2(CO)_3(NCMe)_2]$ (M = Mo, W), after treatment with ammonium diethyldithiophosphate and phosphine under different conditions. The structure of the tungsten complexes was determined by single crystal X-ray diffraction. During the synthesis of **3a**, oxidation of the phosphine took place and a molecule of oxidised phosphine occupies channels in the crystal. DFT/B3LYP calculations on models of **1a** and **2a** showed the capped octahedron structure, observed in most dicarbonyl complexes of this family, to be preferred by 1.4 and 2.6 kcal $mol^{-1}$ for the dppm and the dppe complexes, respectively. Strong steric repulsions can reverse this trend, as happens with the rigid dppm ligand. Complex **1a** adopts a pentagonal bipyramidal geometry, which is often found in related monocarbonyl complexes. © 2002 Elsevier Science B.V. All rights reserved.

*Keywords:* Tungsten; Molybdenum; DFT calculations; Seven coordination; Crystal structures

---

## 1. Introduction

The role of molybdenum in chemistry ranges from its presence in metalloenzymes such as nitrogenase, where it is involved in nitrogen fixation in association with iron [1,2], to industrial processes, among which one of the most relevant is hydrodesulfurisation [3]. A full understanding of the mechanisms of these and other reactions requires a good knowledge of molybdenum chemistry. Molybdenum(II) derivatives have been widely synthesised and characterised [4–6]. Most of the organometallic complexes satisfy the 18 electron rule and are heptacoordinate, although examples of more unusual unsaturated 16 electron carbonyl derivatives have also been described [4h]. The seven-coordinate complexes exhibit the typical structures ranging from the capped octahedron, capped trigonal prism and pentagonal bipyramid, to the 4:3 geometry [4c], which have been studied in detail, as well as their interconversion pathways [7]. Following previous work [8], we describe the synthesis and characterisation of new Mo(II) and W(II) complexes containing carbonyl, iodide, phosphine and dithiophosphate. Some of the compounds have been structurally characterised by single crystal X-ray diffraction. Different structural arrangements are observed in these two groups of compounds, depending on the type of ligands in the coordination sphere of the metal. A rationalisation of the preferences is given based on DFT calculations [9] using the GAUSSIAN 98 program [10].

---

* Corresponding author.
*E-mail address:* mjc@itqb.unl.pt (M.J. Calhorda).

PII: S0020-1693(01)00699-5

## 2. Results and discussion

### 2.1. Chemical results

The complexes $[MI_2(CO)_3(NCMe)_2]$ (M = Mo, W) [4] were treated with ammonium diethyldithiophosphate (1:1), in dichloromethane. After separation of a solid precipitate, phosphine ($Ph_2PCH_2PPh_2$ = dppm or $Ph_2P(CH_2)_2PPh_2$ = dppe) was added to the filtrate to afford new complexes. The product from the reaction of $[WI_2(CO)_3(NCMe)_2]$ with dppe (**1a**) exhibited two $\nu_{C\equiv O}$ stretching modes at 1933 and 1860 $cm^{-1}$, assigned to the symmetric and antisymmetric modes of two coordinated carbonyl groups. The $^1H$ NMR spectrum in $CD_3CN$ shows four groups of peaks, which can be assigned to the phenyl protons of dppe ($\delta = 7.57$ ppm), the methylenic protons of dppe ($\delta = 2.70–2.76$ ppm), the methylenic protons of the ethyl group ($\delta = 3.96–4.06$ ppm) and the methylic protons of the ethyl group ($\delta = 1.24–1.28$ ppm), respectively, integrating approximately as 20:4:4:6, respectively. The structure of **1a** determined using single crystal X-ray diffraction was found to be a heptacoordinate W(II) complex $[WI(CO)_2(dppe)\{S_2P(OEt)_2\}]$. The same reaction was carried out, using dppm as the phosphine. A similar product, **2a**, was obtained, which also exhibited two $\nu_{C\equiv O}$ stretching modes at 1930 and 1847 $cm^{-1}$ and four $^1H$ NMR peaks (multiplets) at $\delta$ 7.55, 5.18–5.26, 4.10 and 1.27–1.32 ppm, for the phenyl and methylene protons of dppm, and methylene and methyl protons of the ethyl groups, respectively. The $^{31}P$ NMR spectrum in $CD_3CN$ showed two peaks at 101.1 and 52.3 ppm, assigned to dppm and $S_2P(OEt)_2$, respectively. The assignment of this complex as $[WI(CO)_2(dppm)\{S_2P(OEt)_2\}]$ was also confirmed by a single crystal X-ray study.

Table 1
Bond lengths (Å) and angles (°) for complex $[WI(CO)_2(dppe)\{S_2P(OEt)_2\}]$ (**1a**)

| | | | |
|---|---|---|---|
| *Bond lengths* | | | |
| W–C(100) | 1.951(12) | W–C(200) | 1.940(16) |
| W–S(11) | 2.619(3) | W–S(13) | 2.599(4) |
| W–P(1) | 2.513(4) | W–P(4) | 2.523(3) |
| W–I | 2.888(3) | | |
| *Bond angles* | | | |
| P(1)–W–P(4) | 76.7(1) | C(100)–M–C(200) | 69.9(6) |
| C(100)–W–P(1) | 80.7(4) | C(200)–W–P(1) | 121.1(4) |
| C(200)–W–P(4) | 75.4(4) | C(100)–W–P(4) | 119.3(3) |
| C(200)–W–S(13) | 124.2(3) | C(100)–W–S(13) | 76.9(4) |
| P(1)–W–S(13) | 95.1(1) | P(4)–W–S(13) | 159.5(1) |
| C(200)–W–S(11) | 73.8(4) | C(100)–W–S(11) | 107.1(4) |
| P(1)–W–S(11) | 165.1(9) | P(4)–W–S(11) | 109.0(1) |
| S(13)–W–S(11) | 74.9(1) | C(200)–W–I | 138.3(4) |
| C(100)–W–I | 151.6(4) | P(1)–W–I | 82.7(1) |
| P(4)–W–I | 78.6(1) | S(13)–W–I | 81.8(1) |
| S(11)–W–I | 84.9(1) | | |

The two reactions described above were repeated starting from the Mo complex $[MoI_2(CO)_3(NCMe)_2]$ and allowing it to react with dppe or dppm, to afford, respectively, $[MoI(CO)_2(dppe)\{S_2P(OEt)_2\}]$ (**1b**) and $[MoI(CO)_2(dppm)\{S_2P(OEt)_2\}]$ (**2b**). The infrared spectra of **1b** also exhibited two $\nu_{C\equiv O}$ stretching modes at 1943 and 1875 $cm^{-1}$, while four peaks could be observed in the $^1H$ NMR spectra in $CD_3CN$. These peaks were assigned to phenyl protons ($\delta = 7.59$ ppm), $CH_2$ from dppe ($\delta = 2.69–2.75$ ppm), $CH_2$ from OEt ($\delta = 3.97–4.02$ ppm) and $CH_3$ from OEt ($\delta = 1.22–1.27$ ppm) and integrated approximately as 20:4:4:6. The structure of complex **1b** therefore was considered to be equivalent to that of the tungsten analogue. Similarly, $[MoI(CO)_2(dppm)\{S_2P(OEt)_2\}]$ (**2b**) exhibited two $\nu_{C\equiv O}$ stretching modes at 1934 and 1859 $cm^{-1}$, as well as four peaks in the $^1H$ NMR spectrum, assigned to phenyl protons ($\delta = 7.22–7.80$ ppm), $CH_2$ from dppm ($\delta = 4.20–4.25$ ppm), $CH_2$ from OEt ($\delta = 3.77–3.99$ ppm) and $CH_3$ from OEt ($\delta = 1.28–1.38$ ppm), integrating as 20:2:4:6, comparable to the W analogue **2a**.

$[MoI_2(CO)_3(NCMe)_2]$ [4] was treated with ammonium diethyldithiophosphate, in dichloromethane. After separation of a solid precipitate, dppe was added to the filtrate and the final product allowed to precipitate during a long period (2 weeks), in order to attempt to form the tungsten analogue of the oxidation product $[Mo(O)(I)(dppe)\{S_2P(OEt)_2\}]$ [8]. The single crystal X-ray determination showed indeed that a new W complex was present $[W(CO)(dppe)\{S_2P(OEt)_2\}_2][O_2dppe]$ (**3a**), along with one molecule of dioxidised dppe. The tungsten complex is the analogue of $[Mo(CO)(dppe)\{S_2P(OEt)_2\}_2]$ (**3b**), previously described, but formed after a relatively fast precipitation [8]. However, while the oxidation took place on the metal for Mo, in the case of tungsten it occurs on the phosphine. The $^1H$ NMR spectrum of **3a** in $CD_3CN$ exhibits peaks assigned to phenyl groups ($\delta = 7.34–7.64$), methylenic ($\delta = 3.89–3.92$, Et; $\delta = 2.71$, dppe) and methylic ($\delta = 1.17–1.29$), but a reliable integration is not possible. One band at 1825 $cm^{-1}$ could be assigned to the $\nu_{C\equiv O}$ stretching.

### 2.2. Crystal structures

The structures of complexes $[WI(CO)_2(dppe)\{S_2P(OEt)_2\}]$ (**1a**), $[WI(CO)_2(dppm)\{S_2P(OEt)_2\}]\cdot 0.25H_2O$ (**2a**) and $[W(CO)(dppe)\{S_2P(OEt)_2\}_2][O_2dppe]$ (**3a**) were determined by single crystal X-ray diffraction.

Bond distances and selected angles in the tungsten coordination are given in Table 1 for complex **1a** and in Table 2 for complexes **2a** and **3a**. The three complexes are all seven coordinate.

An ORTEP diagram of the complex **1**, presented in Fig. 1, shows that two sulfurs from $S_2P(OEt)_2$, one

Table 2
Bond lengths (Å) and angles (°) for complexes [WI(CO)$_2$(dppm){S$_2$P(OEt)$_2$}] (**2a**) and [W(CO)(dppe){S$_2$P(OEt)$_2$}$_2$] (**3a**)

| | | | | | |
|---|---|---|---|---|---|
| *[WI(CO)$_2$(dppm){S$_2$P(OEt)$_2$}] (**2a**)* | | | | | |
| *Bond lengths* | | | | | |
| W–P(1) | 2.493(11) | W–P(3) | 2.562(10) | W–S(11) | 2.605(11) |
| W–C(100) | 1.92(4) | W–C(200) | 1.96(3) | W–S(13) | 2.650(8) |
| W–I | 2.919(4) | | | | |
| *Bond angles* | | | | | |
| P(1)–W–P(3) | 64.4(3) | C(200)–W–P(1) | 71.7(12) | P(3)–W–I | 82.1(3) |
| S(11)–W–I | 81.5(2) | C(200)–W–S(11) | 73.3(11) | C(100)–W–S(13) | 171.2(11) |
| S(11)–W–S(13) | 75.5(3) | C(200)–M–C(100) | 76.2(11) | C(200)–W–S(13) | 111.1(8) |
| C(200)–W–P(3) | 126.6(11) | C(200)–W–I | 142.0(12) | C(100)–W–P(1) | 104.4(12) |
| C(100)–W–S(11) | 102.7(10) | C(100)–W–I | 82.3(10) | C(100)–W–P(3) | 86.5(9) |
| P(1)–W–S(11) | 128.3(3) | P(1)–W–I | 145.0(2) | P(1)–W–S(13) | 83.1(3) |
| P(3)–W–S(11) | 159.9(3) | P(4)–W–S(13) | 92.7(3) | S(13)–W–I | 88.9(2) |
| *[W(CO)(dppe){S$_2$P(OEt)$_2$}$_2$] (**3a**)* | | | | | |
| *Bond lengths* | | | | | |
| W–P(1) | 2.481(4) | W–P(4) | 2.499(3) | W–S(13) | 2.705(4) |
| W–S(11) | 2.582(4) | W–S(21) | 2.609(4) | W–S(23) | 2.608(4) |
| W–C(100) | 1.892(12) | | | | |
| *Bond angles* | | | | | |
| P(1)–W–P(4) | 75.9(1) | S(11)–W–S(23) | 74.0(1) | S(23)–W–S(21) | 73.8(1) |
| P(4)–W–S(11) | 71.8(1) | P(1)–W–S(21) | 71.3(1) | S(21)–W–S(13) | 79.8(1) |
| C(100)–W–S(13) | 169.8(4) | S(11)–W–S(13) | 75.9(1) | S(23)–W–S(13) | 88.9(1) |
| C(100)–W–P(1) | 81.3(4) | C(100)–W–P(4) | 91.5(3) | C(100)–W–S(11) | 95.4(4) |
| C(100)–W–S(23) | 83.5(4) | C(100)–W–S(21) | 104.4(3) | P(1)–W–S(11) | 147.4(1) |
| P(1)–W–S(13) | 109.0(1) | P(1)–W–S(23) | 136.8(1) | P(4)–W–S(13) | 90.9(1) |
| P(4)–W–S(21) | 140.6(1) | P(4)–W–S(23) | 144.8(1) | S(11)–W–S(21) | 139.7(1) |

iodine, two carbonyl groups and two phosphorus from a dppe surround the metal centre in a distorted capped-octahedral coordination environment with a carbonyl C(200)–O(200) in the capping position. The atoms S(11), P(4) and C(100) defined the capped triangular face, while the atoms S(13), P(1) and I define the opposite uncapped face, leading to an angle I–W–C(100) of 151.6(4)°. The two carbonyl groups are bonded linearly to tungsten with W–C–O angles of 175.6(9) and 176.9 (10)°, respectively. This type of geometric arrangement was found for related heptacoordinate isomorphous complexes [M{S$_2$P(OEt)$_2$}$_2$(CO)$_2$(PPh$_3$)] (M = W(II) **4a** or Mo(II) **4b**) and [M(CO)$_2${S$_2$P(OEt)$_2$}$_2$]$_2$(μ-dppe) (M = W(II) **5a** or Mo(II) **5b**). However, in these complexes, the ligands adopt a different disposition around the metal, with a corner of the uncapped triangular face occupied by a sulfur of the S$_2$P(OEt)$_2$ bidentate ligand rather than an iodine. Furthermore, the remaining sulfur of this bidentate ligand substitutes on the equatorial plane a phosphorus of the dppe ligand. In spite of these structural differences, the W–S, W–C and W–P distances in **1a** compare quite well with those found for **4a**, **4b**, **5a** and **5b**.

ORTEP diagrams of the complexes **2a** and **3a** together with the labelling scheme adopted are presented in Figs. 2 and 3, respectively. In contrast with the former structure described, in these two complexes the disposition of the ligands around the metal leads to a coordination sphere which can be described as a distorted bipyramidal pentagon, although **2a** is intermediate between that geometry and the capped octahedron found in **1a**.

Thus, in complex **2b** the equatorial coordination plane contains two phosphorus donors of a dppm ligand, one iodine atom, one carbon atoms from a

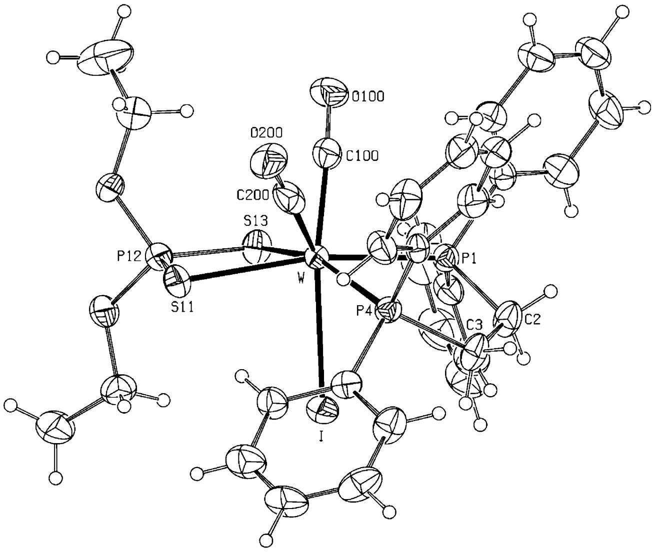

Fig. 1. An ORTEP view of [WI(CO)$_2$(dppe){S$_2$P(OEt)$_2$}] (**1a**) with thermal ellipsoids drawn at 30% probability. The atom numbering scheme of the phenyl and ethoxy groups is omitted for clarity.

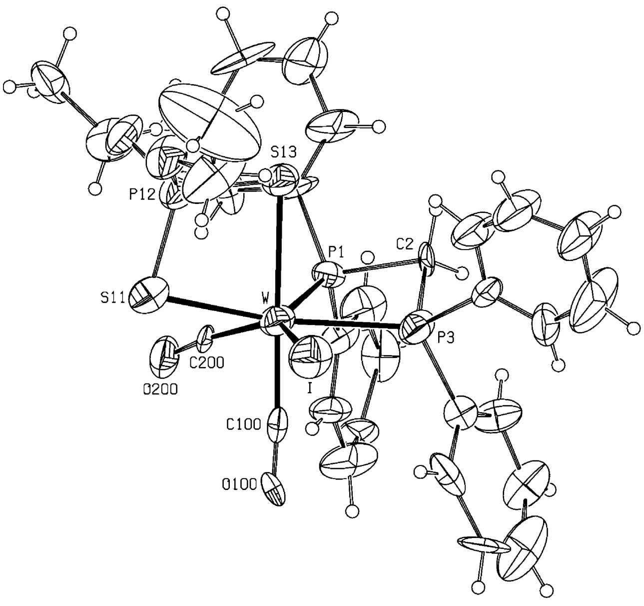

Fig. 2. An ORTEP view of [WI(CO)$_2$(dppm){S$_2$P(OEt)$_2$}] (**2a**). Details were given in Fig. 1.

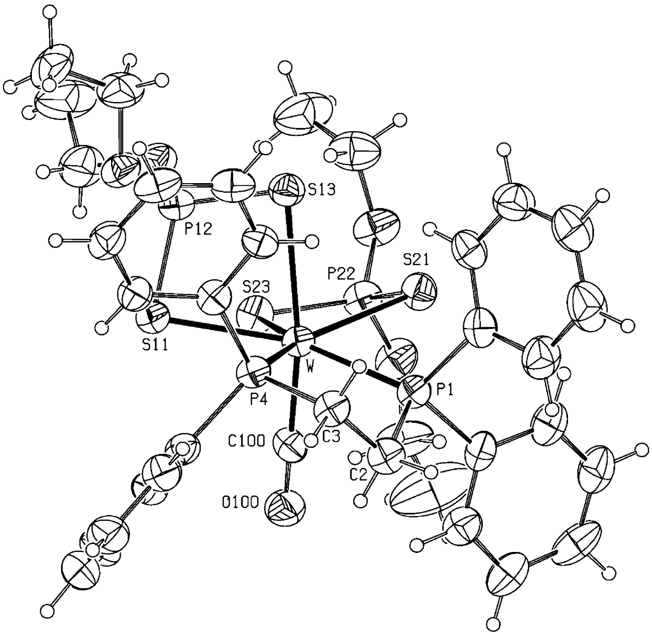

Fig. 3. An ORTEP view of [W(CO)(dppe){S$_2$P(OEt)$_2$}$_2$] (**3a**). Details were given in Fig. 1.

carbonyl group and one sulfur from a S$_2$P(OEt)$_2$ bidentate ligand. In complex **3a**, three sulfurs of two S$_2$P(OEt)$_2$ bidentate ligands and two phosphorus from the dppe ligand determine the equatorial coordination plane. In both complexes, the seven coordination is completed with the remaining sulfur of the dithiolate ligand and a carbonyl group in the axial positions, leading to an angle S(13)–W–C(100) of 171.2(11)° in **2a** and 169.8(4)° in **3**. In both cases the atoms that compose the equatorial coordination plane display a significant deviation from the mean least-squares plane calculated with their atomic positions. These deviations are in Å: 0.437(10) [P(1)], 0.463(12) [S(11)], −0.716(14) [C(200)], −0.138(7) [I] and −0.047(2) [P(3)] in **2a**; 0.529(2) [S(21)], −0.437(2) [S(23)], 0.204(2) [S(11)], −0.396(2) [P(1)] and 0.100(2) [P(4)] in **3a**. However, the *cis* angles subtended at the tungsten centre on the equatorial coordination plane are close to the ideal value of 72° for a perfect bipyramid. The largest shift of this value is 10.1(3)° in **2a** and only of 3.9(1)° in **3**. In both complexes the distortion of the coordination sphere can be ascribed to the steric bulk of the diphenylphosphine ligand, dppm in **2a** or dppe in **3a**. Furthermore, and as would be expected, the P–W–P angle of 64.4(3)° in **2a** is smaller than that of 75.9(1)° in **3a**, since dppm has a smaller bite angle than dppe. In both complexes the Mo–S axial distance is longer than the equatorial ones by approximately 0.10 Å in **3a** and 0.05 Å in **2a**. This is probably due to the fact that the small bite angle of S–P–S of the S$_2$P(OEt)$_2$ ligand prevents sulfur from achieving the ideal position of the bipyramid. Indeed, the angle S$_{ax}$–W–S$_{eq}$ is 75.9(1)° in **3a** and 75.5(3)° in **2a**.

The X-ray structure of the molybdenum analogue of **3a**, [Mo(CO)(dppe){S$_2$P(OEt)$_2$}$_2$] (**3b**) has been reported before [8]. Bond distances and angles are comparable in the metal coordination sphere of both complexes. In the crystal of **3a**, an oxidised O$_2$dppe molecule is located on the crystallographic inversion centre adopting an *anti* conformation with a P–C–C–P torsion angle of 180°. The P–O distance of 1.26(3) Å is consistent with a P=O double bond [11].

The crystal structure of **1a** and **2a** consists of discrete molecules of [WI(CO)$_2$(dppe){S$_2$P(OEt)$_2$}] and [WI(CO)$_2$(dppm){S$_2$P(OEt)$_2$}], respectively. The complex **2a** also contains crystallisation waters with an occupancy factor of 0.25 in its crystal lattice. In both cases, no additional relevant structural features are apparent from their crystal packing diagrams.

In spite of the structural similarity between the structures of the complexes [M(CO)(dppe){S$_2$P(OEt)$_2$}$_2$] (M = W(II) in **3a** and M = Mo(II) in **3b**), they crystallise in different centrosymmetric space groups ($P\bar{1}$ for **3b** and $C2/c$ for **3a**) yielding different packing arrangements. In **3a** the molecular assembly of the [WI(CO)$_2$(dppe){S$_2$P(OEt)$_2$}] molecules affords large open channels running along the *b* crystallographic axis. These channels accommodate the molecules of O$_2$dppe as shown in Fig. 4. No hydrogen bonds were found involving [WI(CO)$_2$(dppe){S$_2$P(OEt)$_2$}] and O$_2$dppe. Therefore, these molecules are aggregated in the crystal only by van der Waals forces.

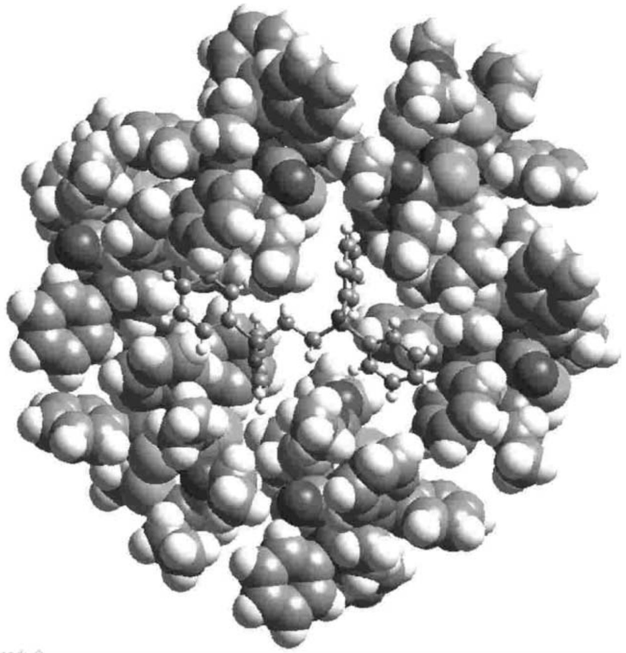

Fig. 4. Crystal packing diagram of [W(CO)(dppe){$S_2P(OEt)_2$}$_2$][$O_2$dppe] (**3a**). View perpendicular to the [010] crystallographic plane, showing how the assembled complex species define the channels, which accommodate $O_2$dppe units. Molecules of complex and $O_2$dppe are represented in the CPK and ball and stick modes, respectively.

### 2.3. Theoretical calculations

DFT calculations [9] were performed using the B3LYP approach within GAUSSIAN 98 [10] on models of complexes **2a** and **1a** where all the ethyl and phenyl groups were replaced by hydrogen atoms, [WI(CO)$_2${$H_2P(CH_2)_nPH_2$}{$S_2P(OH)_2$}] with $n = 1$ (dppm) or 2 (dppe). Complex **2a** was chosen to start the study because it carries the smaller bidentate phosphine dppm, rather than dppe. Preliminary calculations on a much simplified model based on monodentate ligands containing P and S led to no consistent geometries. The optimised geometry of [WI(CO)$_2$($H_2PCH_2PH_2$){$S_2P(OH)_2$}], a pentagonal bipyramid, is shown in Fig. 5a and compared with the X-ray structure (Fig. 5b).

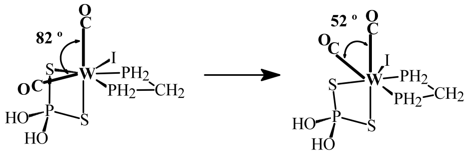

Scheme 1.

There is a good agreement between the calculated and experimental distances, the largest deviations being found for the W–P bonds. A similar agreement is observed for angles. For instance, the calculated P–W–P angle of 66.4° is very similar to the experimental 64.1°. Fig. 5 emphasises the similarities between both structures. The conformation of the W–P–C–P–W cycle, however, differs considerably, the W–P–C–P torsion angle varying from 23.6° in the experimental to −10.6° in the calculated structure. The reason for this difference can be assigned to the presence of the phenyl groups which force a change in chain conformation owing to their bulk. A similar, though less pronounced effect, is observed in the ethyl groups of the sulfur ligand. The possible existence of other isomers was checked, considering that the capped face octahedron was systematically observed in a family of related compounds containing two carbonyl groups [8] and also in the dppe analogue, **1a**. In order to study this transformation, the carbonyl in the equatorial plane of the bipyramid was constrained to move out of that plane by 5° steps (Scheme 1), the geometry being fully optimised for each point. The energy increases by 0.5, 1.6, 3.0, 4.5, 5.8 and 7.7 kcal mol$^{-1}$, respectively, after each

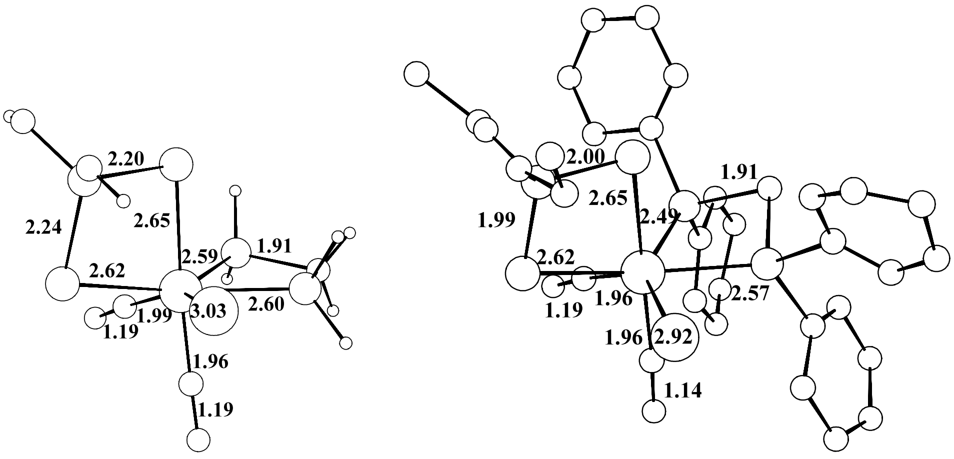

Fig. 5. The structure of model [WI(CO)$_2$($H_2PCH_2PH_2$){$S_2P(OH)_2$}] (**2a**): (a) optimised structure from DFT calculations; (b) X-ray structure. Hydrogen atoms omitted for clarity.

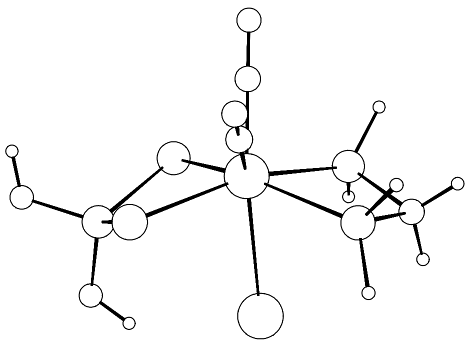

Scheme 2.

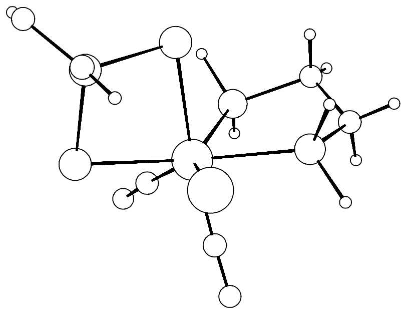

Scheme 3.

step, in a total amount of 23.1 kcal mol$^{-1}$, when the pentagonal bipyramid has become a capped octahedron with a carbonyl as a capping ligand. This structure is therefore not favoured on electronic grounds.

In the structure of **2a** discussed above, the bidentate ligands are orthogonal to each other, leading to a carbonyl *trans* to a sulfur atom rather than to iodine. On the other hand, complex **1a** exhibits a different structural arrangement because the two bidentate ligands, namely the phosphine and the dithiophosphate lie in the same plane (approximately), which is an equatorial plane of either a pentagonal bipyramid or a capped octahedron (as observed). This alternative type of arrangement was also checked for complex **2a** and calculations on a suitable model led to an energy 1.4 kcal mol$^{-1}$ lower (Scheme 2). Notice that this structure is very similar to that observed in the dppe derivative **1a**.

A model was also built for complex **1a** and the geometry optimisation led to a geometry similar to that observed in the X-ray structure, which is shown in Fig. 6a and compared with the experimental one (Fig. 6b).

The calculated distances are a bit longer than the experimental ones, but the agreement is relatively good. The conformations of the R groups are, as expected, not well reproduced by the hydrogen containing models, although the phosphine chain is very similar. Calculations on an isomer having the ligand arrangement of **2a** resulted in a species with an energy higher by 2.6 kcal mol$^{-1}$, shown in Scheme 3.

The previous results indicate that the capped octahedron structure is slightly preferred in both cases, when the bulky Ph and Et groups are not present. This arrangement was found in analogous seven coordinate complexes containing two carbonyls [8]. The energy differences between the two isomers are very small, namely 1.4 and 2.6 kcal mol$^{-1}$ for the dppm and the dppe complexes, respectively, and can easily be overcome when steric repulsions introduced by the substituents are present. The four phenyl groups in the rigid dppm phosphine seem to prevent this arrangement, while dppe, with a longer carbon chain, is more flexible and can adjust.

The pentagonal bipyramidal geometry found in [WI(CO)$_2$(dppm){S$_2$P(OEt)$_2$}] (**2a**) has been associated with monocarbonyl derivatives. The other structurally characterised complex of this work, [W(CO)(dppe){S$_2$P(OEt)$_2$}$_2$] (**3a**) also belongs to this group and exhibits this geometry. It is interesting to notice how the three bidentate ligands are arranged. Two of them occupy four positions of the equatorial plane (as in **1a**), while the third, a dithiophosphate ligand, occupies the fifth position of that plane as well as an axial one, becoming *trans* to the carbonyl (as in **2a**) and orthogonal to the other bidentate ligands.

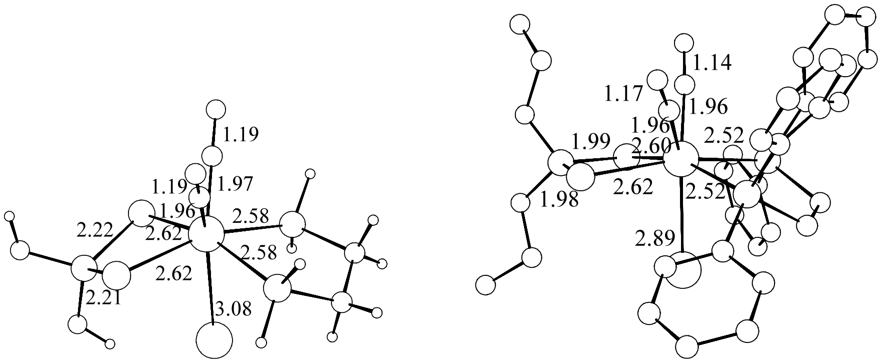

Fig. 6. The structure of model [WI(CO)$_2${H$_2$P(CH$_2$)$_2$PH$_2$}{S$_2$P(OH)$_2$}] (**1a**): (a) optimised structure from DFT calculations; (b) X-ray structure. Hydrogen atoms omitted for clarity.

## 3. Conclusions

New complexes [MI(CO)$_2$(dppe){S$_2$P(OEt)$_2$}] (M = W, **1a**; M = Mo, **1b**), [MI(CO)$_2$(dppm){S$_2$P(OEt)$_2$}] (M = W, **2a**; M = Mo, **2b**) and [W(CO)(dppe){S$_2$P(OEt)$_2$}$_2$][O$_2$dppe] (**3a**) were synthesised and the structure of the W complexes was determined by single crystal X-ray diffraction. The capped octahedron geometry was found for **1a**, while both **2a** and **3a** exhibited a pentagonal bipyramidal arrangement. DFT/B3LYP calculations performed on model complexes of **1a** and **2a** having Ph and Et groups replaced by hydrogen atoms showed similar stabilities for the two isomers of each complex, the capped octahedron being slightly favoured. The experimental observation of the pentagonal bipyramidal structure can be traced to the constraints imposed by the phosphine chelate chain, which force the dppm derivative to adopt such geometry, instead of the capped octahedron, usually preferred in similar dicarbonyl complexes.

## 4. Experimental

### 4.1. Synthesis

Commercially available reagents and all solvents were purchased from standard chemical suppliers. All solvents were used without further purification except acetonitrile (dried over CaH$_2$), dichloromethane (dried over CaH$_2$) and THF, which was distilled over sodium/benzophenone ketyl and used immediately. NH$_4$[S$_2$P(OEt)$_2$] (Aldrich) was recrystallised from THF. The complexes [MI$_2$(CO)$_3$(NCMe)$_3$] (M = Mo, W) were synthesised according to literature procedures [4a].

$^1$H NMR spectra were recorded in a Bruker AMX-300 (300 MHz) spectrometer in d$^3$-CD$_3$CN ($\delta$ 1.93), using TMS as internal reference and $^{31}$P shifts were measured with respect to external 85% H$_3$PO$_4$. Elemental analyses were carried out at ITQB. The IR spectra were recorded in a Unicam Mattson 7000 FTIR spectrometer. Samples were run as KBr pellets.

### 4.2. Preparation of [WI(CO)$_2$(dppe){S$_2$P(OEt)$_2$}] (1a)

[WI$_2$(CO)$_3$(NCMe)$_2$] (0.1208 g, 0.2 mmol) was dissolved in CH$_2$Cl$_2$ (10 ml) and solid NH$_4$[S$_2$P(OEt)$_2$] (0.041 g, 0.2 mmol) was added with vigorous stirring. The colour of the solution changed from dark-red to red and a white precipitate formed gradually in 30 min. The reaction mixture was filtered, solid dppe (0.080 g, 0.2 mmol) was added to the filtrate and the colour of solution quickly turned to orange. The solution was stirred for a further 30 min and then concentrated to about 5 ml. Hexane (20 ml) was added and the mixture was cooled down (− 20 °C) overnight to afford yellow crystals of the product (0.135 g, yield 71%). One of the crystals was suitable for a single crystal X-ray diffraction study.

*Anal.* Calc.: C, 40.41; H, 3.58; S, 6.74. Found: C, 40.36; H, 3.73; S, 6.78%. IR (KBr, $\nu_{C\equiv O}$ cm$^{-1}$): 1933.1, 1860.3. $^1$H NMR (CD$_3$CN, ppm): 7.57 (s, 20H, C$_6$*H*$_5$); 3.96–4.06 (m, 4H, OC*H*$_2$CH$_3$); 2.70–2.76 (m, 4H, C*H*$_2$ from dppe); 1.24–1.28 (m, 6H, OCH$_2$C*H*$_3$).

### 4.3. Preparation of [WI(CO)$_2$(dppm){S$_2$P(OEt)$_2$}] (2a)

[WI$_2$(CO)$_3$(NCMe)$_2$] (0.1208 g, 0.2 mmol) was dissolved in CH$_2$Cl$_2$ (10 ml) and solid NH$_4$[S$_2$P(OEt)$_2$] (0.041 g, 0.2 mmol) was added with vigorous stirring. The colour of the solution changed from dark-red to red and a white precipitated formed gradually. The reaction mixture was then filtered, solid dppm (0.077 g, 0.2 mmol) was added to the filtrate and the solution was stirred for a further 30 min. Hexane (30 ml) was added to the solution and the mixture was kept at 0 °C for 3 days to afford red crystals of the product (0.110 g, yield 59%). One of the crystals was suitable for a single crystal X-ray diffraction study.

*Anal.* Calc.: C, 39.74; H, 3.42; S, 6.84. Found: C, 39.14; H, 3.46; S, 6.60%. IR (KBr, $\nu_{C\equiv O}$ cm$^{-1}$): 1929.5, 1847.3. $^1$H NMR (CD$_3$CN, ppm): 7.55 (s, 20H, C$_6$*H*$_5$); 5.18–5.26 (m, 2H, C*H*$_2$ from dppm); 4.10 (s, 4H, OC*H*$_2$CH$_3$); 1.27–1.32 (m, 6H, OCH$_2$C*H*$_3$). $^{31}$P, 101.1 (P from S$_2$P(OEt)$_2$); 52.3 (P from dppe).

### 4.4. Preparation of [MoI(CO)$_2$(dppe){S$_2$P(OEt)$_2$}] (1b)

[MoI$_2$(CO)$_3$(NCMe)$_2$] (0.1032 g, 0.2 mmol) was dissolved in CH$_2$Cl$_2$ (10 ml) and solid NH$_4$[S$_2$P(OEt)$_2$] (0.041 g, 0.2 mmol) was added with vigorous stirring. The colour of the solution changed from dark-red to red–brown and a white precipitated formed gradually in 30 min. The reaction mixture was then filtered and solid dppe (0.080 g, 0.2 mmol) was added to the filtrate; gas evolution occurred and the colour of the solution changed to red quickly. The solution was stirred for a further 30 min, hexane (20 ml) was added and the mixture was kept at 0 °C for 3 days to afford red crystals of **1b** (0.14 g, yield 81%).

One of the crystals was suitable for a single crystal X-ray diffraction study.

*Anal.* Calc.: C, 44.53; H, 3.94; S, 7.42. Found: C, 44.51; H, 4.14; S, 7.21%. IR (KBr, $\nu_{C\equiv O}$ cm$^{-1}$): 1943.4, 1874.9. $^1$H NMR (CD$_3$CN, ppm): 7.59 (s, 20H, C$_6$*H*$_5$); 3.97–4.02 (m, 4H, OC*H*$_2$CH$_3$); 2.69–2.75 (m, 4H, C*H*$_2$ from dppe); 1.22–1.27 (m, 6H, OCH$_2$C*H*$_3$).

### 4.5. Preparation of [MoI(CO)$_2$(dppm){S$_2$P(OEt)$_2$}] (2b)

This dppm complex was prepared and crystallised in a similar way as described for **2a**. Red–brown crystals were formed (0.09 g, yield 53%).

*Anal.* Calc.: C, 43.86; H, 3.77; S, 7.55. Found: C, 42.57; H, 3.96; S, 7.49%. IR (KBr, $\nu_{C\equiv O}$ cm$^{-1}$): 1934.0, 1859.1. $^1$H NMR (CD$_3$CN, ppm): 7.22–7.80 (m, 20H, C$_6$*H*$_5$); 4.20–4.25 (m, 2H, C*H*$_2$ from dppm); 3.77–3.99 (m, 4H, OC*H*$_2$CH$_3$); 1.28–1.38 (m, 6H, OCH$_2$C*H*$_3$).

### 4.6. Preparation of [W(CO)(dppe){S$_2$P(OEt)$_2$}$_2$][O$_2$dppe] (**3a**)

[WI$_2$(CO)$_3$(NCMe)$_2$] (120.8 mg, 0.2 mmol) was dissolved in CH$_2$Cl$_2$ (10 ml) and solid NH$_4$[S$_2$P(OEt)$_2$] (84 mg, 0.4 mmol) was added with vigorous stirring. The colour of the solution changed from dark-red to orange and a white precipitated formed gradually (30 min). The reaction mixture was filtered, solid dppe (80 mg, 0.2 mmol) was added to the orange filtrate, the solution was stirred for further 30 min, then concentrated to about 3 ml. Hexane (30 ml) was added, the mixture was kept at room temperature and dark-brown crystals appeared after 2 weeks. The yield was 40 mg. One of the crystals was suitable for a single crystal X-ray diffraction analysis.

*Anal.* Calc.: C, 52.10; H, 4.95; S, 9.27. Found: C, 49.68; H, 4.09; S, 9.42%. IR (KBr, $\nu_{C=O}$ cm$^{-1}$): 1825. $^1$H NMR (CD$_3$CN, ppm): 7.34–7.64 (m, C$_6$*H*$_5$), 3.89–3.92 (m, OC*H*$_2$CH$_3$), 2.71 (s, C*H*$_2$C*H*$_2$ from dppe), 1.17–1.29 (m, OCH$_2$C*H*$_3$).

### 4.7. Crystal structure determinations

The crystal data of the complexes **1a**, **2a** and **3a** are given in Table 3, together with refinement details. The X-ray data for all three complexes were collected on a MAR research plate system using graphite Mo Kα radiation at Reading University. The crystals were positioned at 70 mm from the image plate. Ninety-five frames were measured at 2° intervals using an adequate counting time between 2 and 5 min. Data analysis was carried out with the XDS program [12].

The structures were solved by direct methods with the SHELXS program [13]. All non-hydrogen atoms were refined with anisotropic thermal parameters. The hydrogen atoms were introduced in the refinement at the geometric idealised positions giving isotropic thermal parameters equal 1.2 times those of the carbon atom they were attached. An empirical absorption correction was applied to intensities of **1a**, **2a** and **3a** using a version of the DIFABS program modified for image plate geometry [14]. Structures were then refined by full-matrix least-squares on $F^2$ until convergence with SHELXL [15]. The three X-ray determinations showed positive

Table 3
Crystal data and pertinent refinement details for complexes **1a**, **2a** and **3a**

| Compound | **1a** | **2a** | **3a** |
|---|---|---|---|
| Empirical formula | $C_{32}H_{34}IO_4P_3S_2W$ | $C_{31}H_{32.25}IO_{4.25}P_3S_2W$ | $C_{48}H_{56}O_6P_5S_4W$ |
| Formula weight | 950.37 | 940.60 | 1195.87 |
| Crystal system | monoclinic | orthorhombic | monoclinic |
| Space group | $P2_1/n$ | *Pbcn* | $C2/c$ |
| *Unit cell dimensions* | | | |
| $a$ (Å) | 18.248(23) | 12.147(15) | 32.340(37) |
| $b$ (Å) | 10.988(14) | 16.937(23) | 11.113(14) |
| $c$ (Å) | 19.219(24) | 37.297(38) | 33.983(38) |
| $\alpha$ (°) | | | |
| $\beta$ (°) | 113.34(1) | | 117.96(1) |
| $\gamma$ (°) | | | |
| $V$ (Å$^3$) | 3538 | 7673 | 10788 |
| $Z$ | 4 | 8 | 8 |
| Calculated density (Mg m$^{-3}$) | 1.784 | 1.628 | 1.473 |
| $F$(000) | 1848 | 3650 | 4840 |
| Absorption coefficient (mm$^{-1}$) | 4.425 | 4.081 | 2.489 |
| Theta range (°) | 1.98 to 25.88 | 2.00 to 25.56 | 1.36 to 26.09 |
| Index ranges *hkl* | $-20\leq h\leq 20$, $0\leq k\leq 13$, $-22\leq l\leq 22$ | $0\leq h\leq 14$, $-11\leq k\leq 8$, $-37\leq l\leq 44$ | $-39\leq h\leq 39$, $-13\leq k\leq 13$, $-40\leq l\leq 40$ |
| Reflections collected | 5751 | 6399 | 31504 |
| Unique reflections [$R_{int}$] | 4292 [0.0496] | 2796 [0.1117] | 10116 [0.1292] |
| Data/restraints/parameters | 4292/0/390 | 2796/30/386 | 10116/0/582 |
| Final $R$ indices [$I>2\sigma(I)$] | $R_1=0.0474$, $wR_2=0.1298$ | $R_1=0.0901$, $wR_2=0.2239$ | $R_1=0.0875$, $wR_2=0.2216$ |
| $R$ indices (all data) | $R_1=0.0707$, $wR_2=0.1418$ | $R_1=0.1459$, $wR_2=0.2515$ | $R_1=0.1246$, $wR_2=0.2516$ |
| Goodness-of-fit on $F^2$ | 1.113 | 1.078 | 1.104 |
| Largest difference peak and hole (e Å$^{-3}$) | 1.230 and −0.908 | 1.061 and −0.761 | 1.604 and −1.650 |

peaks for residual electronic density greater than 1 e Å$^{-3}$, but in all cases the corresponding peak was within the metal coordination sphere. ORTEP plots were drawn with the PLATON graphical interface [16] while the crystal packing diagram were performed with CERIUS2 software [17].

### 4.8. DFT calculations

The geometry optimisations were accomplished by means of ab initio and DFT calculations performed with the GAUSSIAN 98 program [10]. The B3LYP hybrid functional with a standard LanL2DZ basis set [18] was used in all calculations. That functional includes a mixture of Hartree–Fock [19] exchange with DFT [9] exchange-correlation, given by Becke's three parameter functional [20] with the Lee, Yang and Parr correlation functional, which includes both local and non-local terms [21]. All the optimised geometries are the result of full optimisations without any symmetry constraints. The starting points for the optimisations were model complexes based on the X-ray structures quoted along the text, with hydrogen atoms replacing the ethyl and phenyl groups.

## 5. Supplementary material

Crystallographic data for the structural analysis have been deposited with the Cambridge Crystallographic Data Centre, CCDC Nos. 165015–165017 for compounds **1a**, **2b** and **3a**, respectively. Copies of this information may be obtained free of charge from The Director, CCDC, 12 Union Road, Cambridge, CB2 1EZ, UK (fax: +44-1223-336-033; e-mail: deposit@ccdc.cam.ac.uk or www: http://www.ccdc.cam.ac.uk).

## Acknowledgements

We thank Zara Miravent Tavares for the elemental analysis (ITQB). H.L. thanks Praxis XXI for a postdoctoral grant. V.F. thanks FCT for a sabbatical leave grant. The University of Reading and EPSRC are thanked for funds for the Image Plate system.

## References

[1] (a) J. Kim, D.C. Rees, Science 257 (1992) 1677;
(b) W.-H. Orme-Johnson, Science 257 (1992) 1639;
(c) J. Kim, D.C. Rees, Nature 360 (1992) 553.

[2] J.J.R. Fraústo da Silva, R.J.P. Williams, The Biological Chemistry of the Elements, Clarendon Press, Oxford, 1991.

[3] H. Topsøe, B.S. Clausen, F.E. Massoth, Hydrotreating Catalysis, in: J.R. Anderson, M. Boudart (Eds.), Catalysis—Science and Technology, vol. 11, Springer, Berlin, 1996.

[4] (a) P.K. Baker, A. Bury, J. Organometal. Chem. 359 (1989) 189;
(b) P.K. Baker, M. van Kampen, D. ap Kendrick, J. Organometal. Chem. 421 (1991) 241;
(c) P.K. Baker, M.B. Hursthouse, A.I. Karaulov, A.J. Lavery, K.M. Abdul Malik, D.J. Muldoon, A. Shawcross, J. Chem. Soc., Dalton Trans. (1994) 3493;
(d) P.K. Baker, A.I. Clark, M.G.B. Drew, M.C. Currant, R.L. Richards, Polyhedron 17 (1998) 1407;
(e) N.G. Aimeloglu, P.K. Baker, M.M. Meehan, M.G.B. Drew, Polyhedron 17 (1998) 3455;
(f) P.K. Baker, L.A. Latif, M.M. Meehan, S. Zanin, M.G.B. Drew, Polyhedron 18 (1999) 257;
(g) P.K. Baker, M.G.B. Drew, A.W. Johans, U. Haas, L.A. Latif, M.M. Meehan, S. Zanin, J. Organometal. Chem. 590 (1999) 77–87;
(h) P.K. Baker, A.I. Clark, M.G.B. Drew, M.C. Durrant, R.L. Richards, Inorg. Chem. 38 (1999) 821.

[5] (a) G. Barrado, D. Miguel, J.A. Pérez-Martinez, V. Riera, J. Organometal. Chem. 463 (1993) 127–133;
(b) G. Barrado, D. Miguel, S. García-Granda, V. Riera, J. Organometal. Chem. 489 (1995) 129–135;
(c) G. Barrado, M.M. Hricko, D. Miguel, V. Riera, H. Wally, S. García-Granda, Organometallics 17 (1998) 820–826.

[6] (a) B. Zhuang, L. Huang, L. He, Y. Yuang, J. Lu, Inorg. Chim. Acta 145 (1988) 225–229;
(b) K.-B. Shiu, S.-M. Peng, M.-C. Cheng, S.-L. Wang, F.-L. Liao, J. Organometal. Chem. 461 (1993) 111–116;
(c) M. Cano, M. Panizo, J.A. Campo, J. Tornero, N. Menéndez, J. Organometal. Chem. 463 (1993) 121–125;
(d) K.-H. Yih, G.-H. Lee, Y. Wang, J. Organometal. Chem. 588 (1999) 125–133.

[7] (a) M.G.B. Drew, Seven-coordination Chemistry, in: Stephen J. Lippard (Ed.), Progress in Inorganic Chemistry, vol. 23, Wiley, New York, 1977;
(b) R. Hoffmann, B.F. Beier, E.L. Muetterties, A.R. Rossi, Inorg. Chem. 16 (1977) 511.

[8] H. Liu, V. Félix, M.G.B. Drew, M.J. Calhorda, J. Organomet. Chem. 632 (2001) 175.

[9] R.G. Parr, W. Yang, Density Functional Theory of Atoms and Molecules, Oxford University Press, New York, 1989.

[10] M.J. Frisch, G.W. Trucks, H.B. Schlegel, G.E. Scuseria, M.A. Rob, J.R. Cheeseman, V.G. Zakrzewski, J.A. Montgomery Jr., R.E. Stratmann, J.C. Burant, S. Dapprich, J.M. Millam, A.D. Daniels, K.N. Kudin, M.C. Strain, O. Farkas, J. Tomasi, V. Barone, M. Cossi, R. Cammi, B. Mennucci, C. Pomelli, C. Adamo, S. Clifford, J. Ochterski, G.A. Petersson, P.Y. Ayala, Q. Cui, K. Morokuma, D.K. Malick, A.D. Rabuck, K. Raghavachari, J.B. Foresman, J. Cioslowski, J.V. Ortiz, A.G. Baboul, B.B. Stefanov, G. Liu, A. Liashenko, P. Piskorz, I. Komaromi, R. Gomperts, R.L. Martin, D.J. Fox, T. Keith, M.A. Al-Laham, C.Y. Peng, A. Nanayakkara, C. Gonzalez, M. Challacombe, P.M.W. Gill, B. Johnson, W. Chen, M.W. Wong, J.L. Andres, C. Gonzalez, M. Head-Gordon, E.S. Replogle, J.A. Pople, GAUSSIAN 98, Revision A.7, Gaussian, Inc., Pittsburgh PA, 1998.

[11] F.H. Allen, J.E. Davies, J.J. Galloy, O. Johnson, O. Kennard, C.F. Macrae, E.M. Mitchell, G.F. Mitchel, J.M. Smith, D.G. Watson, J. Chem. Inf. Comput. Sci. 31 (1991) 187.

[12] W. Kabsch, J. Appl. Crystallogr. 21 (1988) 916.

[13] G.M. Sheldrick, Acta Crystallogr., Sect. A 46 (1990) 467 (SHELXS-86).

[14] N. Walker, D. Stuart, Acta Crystallogr., Sect. A 39 (1983) 158 (DIFABS).

[15] G.M. Sheldrick, SHELX-97, University of Göttingen, Göttingen, Germany, 1997.

[16] A.L. Spek, PLATON, A Multipurpose Crystallographic Tool, Utrecht University, Utrecht, The Nethelands, 1999.

[17] CERIUS2, version 3.5, Molecular Simulations Inc, San Diego, CA, 1997.

[18] (a) T.H. Dunning Jr., P.J. Hay III, in: H.F. Schaefer III (Ed.), Modern Theoretical Chemistry, vol. 3, Plenum Press, New York, 1976, p. 1;

(b) P.J. Hay, W.R. Wadt, J. Chem. Phys. 82 (1985) 270;

(c) W.R. Wadt, P.J. Hay, J. Chem. Phys. 82 (1985) 284;

(d) P.J. Hay, W.R. Wadt, J. Chem. Phys. 82 (1985) 2299.

[19]W.J. Hehre, L. Radom, P.v.R. Schleyer, J.A. Pople, Ab Initio Molecular Orbital Theory, Wiley, New York, 1986.

[20]A.D. Becke, J. Chem. Phys. 98 (1993) 5648.

[21](a) C. Lee, W. Yang, R.G. Parr, Phys. Rev. B 37 (1988) 785;
(b) B. Miehlich, A. Savin, H. Stoll, H. Preuss, Chem. Phys. Lett. 157 (1989) 200.